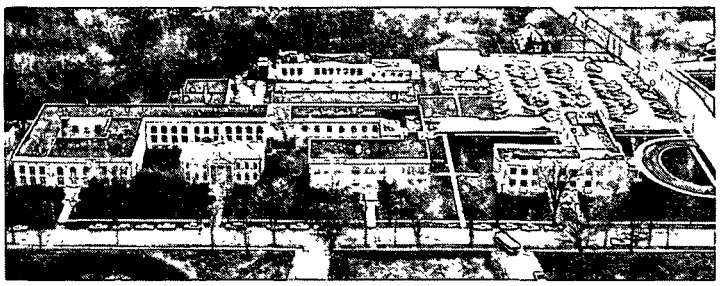

THE INSTITUTE OF PAPER CHEMISTRY, APPLETON, WISCONSIN

IPC TECHNICAL PAPER SERIES
NUMBER 117

MEASUREMENT OF THE ORTHOTROPIC ELASTIC CONSTANTS OF PAPER

G. A. BAUM, C. C. HABEGER, AND E. H. FLEISCHMAN

NOVEMBER, 1981

Measurement of the Orthotropic Elastic Constants of Paper

G. A. Baum, C. C. Habeger, E. H. Fleischman
The Institute of Paper Chemistry

ABSTRACT

A wave theory describing paper as a three-dimensional homogeneous orthotropic plate is discussed, and the theory compared with experiment. The results indicate that as long as the wavelength is large compared to typical fiber dimensions, paper may be considered to behave as a homogeneous orthotropic plate. This allows determination of all nine orthotropic elastic constants.

Measurement of the three Young's moduli, the in-plane shear modulus, and the in-plane Poisson ratios were made as functions of fiber orientation, wet straining, and density. Qualitatively, the results show that a variable producing a change in properties in one direction, alters the properties in the other two directions in a predictable way. The in-plane shear modulus and the Poisson ratios, expressed as $(\nu_{xy}\nu_{yx})^{1/2}$, were found to be relatively insensitive to fiber orientation and wet straining, except at the highest levels of each.

INTRODUCTION

Paper is a layered structure which is highly anisotropic. In the plane of the paper, Young's modulus in the machine direction is typically twice that of the cross-machine direction. This anisotropy results from an increased fiber orientation in the machine direction as well as the effect of drying restraints in this direction. The out-of-plane, or z-direction, Young's modulus, is considerably smaller than the in-plane values, presumably because of the layered structure.

Taken together, the above observations suggest that paper may be described as a three dimensional orthotropic material, that is, a material having three mutually perpendicular symmetry planes. The normal directions to these planes would be the machine direction (MD), cross-machine direction (CD), and the thickness direction (ZD). An orthotropic material is characterized by nine independent elastic constants: three Young's moduli; three shear moduli, and three Poisson ratios.

This article demonstrates that paper may be considered a three-dimensional orthotropic material as far as wave propagation techniques are concerned, and discusses how the orthotropic elastic constants can be measured. These constants are examined with respect to the effects of machine and process variables.

WAVE PROPAGATION IN PAPER

In an isotropic material of infinite extent, two types of wave motion can exist. These are longitudinal (or dilatational) modes, in which the particles composing the material are displaced parallel to the direction of wave propagation, and shear (or distortional) modes in which the particles are displaced perpendicular to the direction of propagation. Longitudinal modes travel faster than shear modes. Both types of waves are nondispersive, that is, the velocity of the wave is not a function of frequency.

If either mode is reflected from a free boundary, however, partial mode conversion occurs. The boundaries in the ZD of paper, for example, couple the two types of waves such that pure bulk modes do not exist (except a shear mode polarized in

the plane of the sheet). An otherwise infinite material that is finite in one dimension is called a plate. It will be shown that paper can be considered a plate-like material as far as elastic wave propagation is concerned.

Wave Propagation in Infinite Media

Before turning our attention to orthotropic plates (i.e., paper), it will be beneficial to consider wave propagation in an infinite orthotropic medium. For such a material the stresses, τ_{ij}, can be expressed in terms of the strain, ε_{ij} by

$$\begin{aligned}
\tau_{11} &= C_{11}\varepsilon_{11} + C_{12}\varepsilon_{22} + C_{13}\varepsilon_{33} \\
\tau_{22} &= C_{12}\varepsilon_{11} + C_{22}\varepsilon_{22} + C_{23}\varepsilon_{33} \\
\tau_{33} &= C_{13}\varepsilon_{11} + C_{23}\varepsilon_{22} + C_{33}\varepsilon_{33} \\
\tau_{23} &= 2C_{44}\varepsilon_{23} \\
\tau_{13} &= 2C_{55}\varepsilon_{13} \\
\tau_{12} &= 2C_{66}\varepsilon_{12}
\end{aligned} \tag{1}$$

The nine elastic stiffnesses, C_{ij} have units of stress (Pa).

In paper we assume the MD, CD, and ZD are the three principal directions of symmetry, 1, 2, and 3, respectively. The strains may be defined in terms of the particle displacements from equilibrium by

$$\varepsilon_{ij} = (U_{i,j} + U_{j,i})/2, \qquad i,j = 1,2,3 \tag{2}$$

where $U_{i,j} = \partial U_i/\partial X_j$.

The equations of motion for mechanical disturbances in an elastic medium are

$$\sum_{j=1}^{3} \tau_{ij,j} = \rho \ddot{U}_i, \qquad i = 1,2,3 \tag{3}$$

where ρ is the mass density of the medium and $\ddot{U}_i = \partial^2 U_i/\partial t^2$.

Substitution of Equations (1) and (2) into (3) yields,

$$\begin{aligned}
\rho\ddot{U}_1 &= C_{11}U_{1,11} + C_{12}U_{2,12} + C_{13}U_{3,13} + C_{55}(U_{1,33} + U_{3,31}) + C_{66}(U_{1,22} + U_{2,21}) \\
\rho\ddot{U}_2 &= C_{12}U_{1,21} + C_{22}U_{2,22} + C_{23}U_{3,23} + C_{44}(U_{2,33} + U_{3,32}) + C_{66}(U_{1,12} + U_{2,11}) \\
\rho\ddot{U}_3 &= C_{13}U_{1,31} + C_{23}U_{2,32} + C_{33}U_{3,33} + C_{44}(U_{2,23} + U_{3,22}) + C_{55}(U_{1,13} + U_{3,11})
\end{aligned} \tag{4}$$

where $U_{i,jk} = \partial^2 U_i/\partial X_j \partial X_k$.

Plane waves are solutions to these equations,

$$U_i = U_{io} \exp\,[\underline{i}(K_x X_1 + K_y X_2 + K_z X_3 - \omega t)], \tag{5}$$

where U_{io} is the oscillation amplitude, K_x,K_y, and K_z are the components of the wave vector $\vec{K}$, ω is the angular frequency, and $\underline{i} = (-1)^{1/2}$.

Solution of Equations (4) give the elastic stiffnesses of the material in terms of measurable velocities. For example, for the infinite orthotropic material, the propagation of longitudinal modes along the three principal directions would give

$$V_{Lx} \ (=\omega/K_x) = (C_{11}/\rho)^{1/2}$$
$$V_{Ly} \ (=\omega/K_y) = (C_{22}/\rho)^{1/2} \qquad (6)$$
$$V_{Lz} \ (=\omega/K_z) = (C_{33}/\rho)^{1/2}$$

While the propagation of shear modes along the principal directions would give in the yz, xz, and xy planes

$$V_{Syz} = (C_{44}/\rho)^{1/2}$$
$$V_{Sxz} = (C_{55}/\rho)^{1/2} \qquad (7)$$
$$V_{Sxy} = (C_{66}/\rho)^{1/2}$$

The relationships between velocities and the off-diagonal elastic stiffnesses C_{12}, C_{13}, and C_{23} [see Equation (1)], involve the propagation of waves not along the principal directions, and are, therefore, more complicated than Equations (6) and (7) above. The determinations of these for paper fall outside of infinite media theory and have been discussed elsewhere (5).

For orthotropic bulk waves traveling in principal directions the particle displacements are normal or parallel to the propagation direction and the waves are not dispersive. In the more general case in which the direction of propagation is not along a principal direction, the particle displacements are not parallel or perpendicular to the propagation direction (1). These waves are still not dispersive, but velocity and the angle between the wave vector and the polarization depend on the propagation direction.

Plate Wave Theory Applied to Paper

Because paper is very thin it cannot be described in terms of an infinite media model. It is reasonable to assume that we must treat it as a plate. A detailed description of the appropriate theory has been presented elsewhere (2). The basic elements can be understood by reference to Figure 1. The normal modes of oscillation in a plate can be expressed as a sum of two shear waves and two longitudinal waves. All four bulk waves have the same vector projected along the plate, but the transverse components are positive for one pair of shear and longitudinal waves, and negative for the other pair. The magnitudes and directions of the waves are chosen so that the free boundary conditions are met at the plate surfaces. Since the shear wave is slower, its direction of propagation is nearer the plate normal. Along the plate, the plate waves are plane waves with a phase velocity equal to the angular frequency divided by the component of the bulk wave vector along the plate. As the frequency changes, a corresponding change in direction of the bulk waves is required in order to satisfy the boundary conditions. Plate waves, then, are dispersive; the velocity is a function of frequency. Plate waves are described as symmetric or antisymmetric, depending on the symmetry about the midplane of the particle displacement along the plate, as shown in Figure 2.

[Figures 1 and 2 here]

A test of the orthotropic plate wave theory (2) was carried out by performing the following steps.

(1) The bulk orthotropic elastic constants, as defined by Equations (6) and (7) were measured for paper using specially constructed samples which approximate the infinite media requirement. The off-diagonal stiffnesses C_{13} and C_{23} were obtained using relationships obtained from orthotropic plate wave theory in the limit as frequency goes to zero and C_{12} was found by propagating a shear wave at 45° to the MD in the MD-CD plane (3). Measurement of the bulk elastic constants required a number of different transducer-specimen configurations as indicated in Figure 3.

[Figure 3 here]

(2) The orthotropic elastic constants determined in Step 1 were used in the plate wave theory to predict the dispersion curves relating phase velocity and frequency. Figure 4 shows dispersion curves for the ZD-MD and ZD-CD planes of a chip board sample. The rapid drop of the zeroth order symmetric, S_o, mode velocity with frequency results from the extremely low value for the measured z-direction stiffness, C_{33}. If this number increased, the drop off would occur at higher frequencies, the higher order modes would begin to propagate at higher frequencies, and the A_o mode would reach a plateau at higher frequencies. An interesting result is the development of "plateaus" in the higher order symmetric modes. These are nearly nondispersive regions at approximately the same velocity as the low frequency S_o mode.

[Figure 4 here]

(3) The final test of the theory and the validity of the measurements of bulk orthotropic elastic constants was performed by measuring plate wave velocities as a function of frequency directly on the paperboard sample. The method of Luukkala et al. (4) was used in which a noncontacting ultrasonic transmitter is used to excite plate modes in the paper. At certain combinations of frequency and orientation of the transmitter, plate waves are excited and a receiver located behind the paper and opposite the transmitter records a maximum signal. The frequency and angular orientation of the transmitter with respect to the paper allow the plate wave velocities to be calculated. These plate velocities can be compared to the plate velocities predicted from theory and bulk constants. Figure 5 shows such a comparison for carton stock. Although the data fall in a narrow frequency "window" (because of limitations due to the air), the agreement between "experiment" and "theory" is very good. The good agreement leads to the following conclusions concerning wave theories applied to paper.

- Paper behaves as a homogeneous continuum,
- The orthotropic description of paper is valid, and
- The bulk orthotropic constants form a self consistent set.

[Figure 5 here]

Subsequent study has verified the existence of the plateaus (5) and led to alternate means of determining the constants C_{11} and C_{22}. The nine orthotropic elastic constants for the carton stock mentioned above have been presented elsewhere

Limitations of Plate Wave Theory Applied to Paper

There are several important limitations on the theory. First, it will not apply for all wavelengths. As the frequency increases, the wavelength becomes shorter. When the measuring wavelength becomes comparable to fiber dimensions the theory is no longer applicable. This occurs in the vicinity of 2 MHz. Second, the theory was developed for an elastic material, while paper is known to be viscoelastic (6). Although a viscoelastic theory would be desirable, the present theory is capable of providing information on elastic response that cannot be found via the more usual mechanical test methods. Finally, as in any wave phenomena, interference and diffraction effects may occur which can cause experimental difficulties. In our work we have found that measurement schemes in which the transducers are closer than approximately one-half wavelength result in undesirable effects. ZD measurements are especially susceptible to such errors because paper is so thin. The errors depend inversely on the paper thickness and measuring frequency. Above approximately 0.5 mm, at 1 MHz, the error is negligible.

ORTHOTROPIC ELASTIC CONSTANTS OF PAPER

The application of ultrasonic techniques to determine the orthotropic elastic constants of paper is part of a fundamental research program in our laboratory. Initial efforts centered on measuring the in-plane (MD-CD) elastic constants of handsheets and machine-made paper. The in-plane constants, in engineering terminology (9), are the two Young's moduli, E_x and E_y, the shear modulus, G_{xy}, and the Poisson ratios, ν_{xy} and ν_{yx}. Since $\nu_{yx} = \nu_{xy}E_x/E_y$, there are only four independent constants. Some of this work has been described elsewhere (7, 8).

Measurements on Mechanically Strained Sheets

The theoretical relationships between ultrasonic velocities and the elastic moduli of paper have been developed for unstrained sheets, and all of our reported laboratory results are for measurements on unstrained sheets. The effects of straining the sheet on the in-plane velocities, however, have been studied, and the results are presented here.

Ultrasonic velocities were measured during mechanical load-elongation tests and during long-term stress relaxation. The experiments were carried out on 30.5 cm (CD) by 200 cm (MD) samples of a bleached ledger paper of basis weight 79 g/m^2. The IPC large scale tensile tester was used to apply uniaxial MD stresses and record the load-elongation behavior. Tests were conducted at relative humidities of 15, 48, 66, and 80%, all at 22.8°C. At each humidity the samples were strained to about 80% of their ultimate tensile strength in four approximately equal stress increments. The ultrasound velocities for longitudinal and shear waves were measured at each increment for both the MD and CD (V_{Lx}, V_{sx}, V_{Ly}, V_{sy}). These measurements were repeated as the specimen was unloaded in four increments. The time required for measurements at each stress increment was about 60 seconds, and of course, stress relaxation did occur in this time.

Stress relaxation effects were investigated by stressing specimens to 80% of ultimate strength, maintaining the strain, and measuring the ultrasonic velocities at times of 1, 22, 90, 162, and 430 hours (all at 48% RH, 22.8°C). Because more time was available for these measurements, they were performed in the usual manner in which a relatively large area of the specimen is examined (8).

The essential results for the load-elongation studies and the stress relaxation studies are given in Tables I and II, respectively. In Table I, conditions at the maximum loads only are shown for each of the relative humidites. The greatest effect is on the MD longitudinal velocity at 80% RH, where the velocity has increased over 6%. At this point the tangent modulus from the load-elongation curve has decreased to about one-third its original value. Thus, even though the samples are not behaving elastically in the mechanical measurements, the ultrasonic velocities differ from their unstrained values by a few percent. The effect on the other two velocities is considerably smaller.

[Tables I and II here]

From Table II it can be seen that the effect of stress relaxation at constant strain is very small for V_{Lx}. Velocity changes due to stress relaxation were less than 1.2% over the 430-hour experiment, while the load decreased over 30%. Velocities V_{Ly} and V_{sx} or V_{sy} were not appreciably affected by the stress relaxation phenomena.

Taken together, the above results suggest that the mechanisms governing the stress-strain relationship at high frequencies are largely independent of the relatively long time phenomena exhibited in the usual stress-strain response. That is, (except for the corrections of the order of the strain) ultrasonic and mechanical deformations superimpose linearly even as mechanical failure is approached. Similar results are found for high frequency mechanical cycling about a point on the stress-strain curve in the plastic regime, although in that case the measured modulus would be less than in the ultrasonic case.

Effect of Fiber Orientation and Wet Straining on Elastic Properties

With increasing confidence in determining the elastic constants of paper by ultrasonic pulse propagation techniques, it was decided to use this new tool to explore the effects of certain papermaking variables. In particular, the effects of fiber orientation and wet straining (or drying restraint) on the measured elastic constants were investigated.

The final properties of paper made from a given furnish can be altered quite dramatically by varying the fiber orientation in the plane of the sheet, and/or varying the restraint imposed on the sheet as it dries. The effect of these variables, individually or together, on the mechanical properties of paper has been the subject of many published articles (10-22). Due to limitations of available testing methods, however, all of these studies were concerned with the in-plane characteristics of the sheet. Most investigations were concerned with only two of the four in-plane elastic constants of paper, namely, Young's modulus in the machine and cross-machine directions.

Our objective was to obtain data showing the effects of fiber orientation and drying restraint on all four of the in-plane elastic moduli (E_x, E_y, G_{xy}, and ν_{xy}). Furthermore, because there is a growing awareness that paper must be considered a three-dimensional material, a second objective was to investigate the effects of in-plane fiber orientation and drying restraints on the ZD elastic stiffness, C_{33}. One conclusion of our earlier experimental work was that the out-of-plane elastic constants of paper could be accurately determined, provided that the sheet thickness is greater than about 0.5 mm.

Three sets of sheets were prepared, one set of random (nonoriented) handsheets and two sets of oriented sheets. All sheets were made from a bleached western softwood kraft pulp, obtained in dry-lap form. Prior to sheet forming, the pulp was soaked, defibered, and beaten in a laboratory Valley beater to a freeness of approximately 500 CSF. The random sheets were formed on an 8 inch by 8 inch Noble and Wood sheet mold and the oriented sheets were formed on a "Formette Dynamique" sheet machine made by Allimand (23, 24). Weyerhaeuser Company generously allowed the use of their machine for making the oriented sheets. Two degrees of fiber orientation, designated as "low" and "high," were achieved by appropriate adjustments of the stock jet velocity and wire speed on the Formette.

Since accurate z-direction measurements require thick sheets, all of the sheets were formed with a basis weight of about 400 g/m^2. These heavy sheets can be formed in a single layer on the Formette with little difficulty. The random handsheets, however, were formed by wet pressing together six sheets, each with a basis weight of about 65 g/m^2, in order to obtain more uniform sheet properties at the required basis weight.

It is well known from a theoretical as well as a practical standpoint, that paper properties vary considerably as a function of the final apparent density of the sheet. Since process conditions, adjusted to produce sheets with different fiber orientations and drying restraints, often result in changing the apparent density as well, it was necessary to include apparent density as a variable. The apparent density was varied by applying different wet pressing pressures with a platen type press.

After wet pressing, the sheets were dried under one of the three levels of controlled restraint. The lowest level involved clamping the sheet biaxially using two pairs of clamps and drying it without allowing any dimensional change. For the medium and high levels of restraint, the sheet was clamped in the direction of preferred fiber orientation (hereafter the MD) and then strained while still wet to about 1.2 or 2.4% strain, respectively, at a rate of about 0.8%/min. When strained in the machine direction, the wet sheet contracted in the cross direction. After wet straining, the sheet also was clamped in the cross direction, allowing no further dimensional change during drying.

The in-plane elastic constants and the z-direction stiffness were determined by ultrasonic techniques as discussed earlier. In addition, Young's modulus in the machine and cross-machine directions were determined "mechanically" on the Instron Universal Testing Machine. The tensile strengths in the machine, cross-machine and z-direction were also measured.

The dependence of the machine direction Young's modulus determined ultrasonically, as a function of fiber orientation, wet straining, and apparent density is shown in Figure 6. The three solid lines correspond to the three different fiber orientations with no wet straining. The lowest solid line is for the random handsheets while the uppermost solid line corresponds to the most oriented sheets. The dashed lines correspond to the maximum wet straining. Fiber orientation has a rather dramatic effect on the modulus, increasing it about 70% over the range investigated. Wet straining has a significant but smaller effect. At each fiber orientation level, wet straining increased the modulus an additional 25%. As more fibers are oriented in the machine direction, the CD Young's modulus decreases quite significantly, as shown in Figure 7. The CD modulus is further decreased by wet straining in the MD. The results for Young's moduli measured mechanically were

qualitatively the same as the ultrasonic results. The mechanically measured Young's moduli are directly proportional to the moduli measured ultrasonically, essentially independent of fiber orientation, wet pressing, and only slightly affected by wet straining.

[Figures 6 and 7 here]

The tensile strength results, presented in Figures 8 and 9, are similar to the results for the moduli except that wet straining has a smaller effect on the tensile strength than on Young's modulus. The observed dependence of the in-plane Young's moduli and tensile strengths on fiber orientation and wet straining is consistent with earlier published work.

[Figures 8 and 9 here]

The dependence of the in-plane shear modulus, G_{xy}, on the three variables investigated is shown in Figure 10. The three solid lines correspond to the three fiber orientations. G_{xy} decreases with increasing fiber orientation, although the effect is considerably smaller than the changes observed for the in-plane Young's moduli. The effect of wet straining on G_{xy} is negligible for the random and slightly oriented sheets, as can be seen in the open and closed symbols on each line, corresponding to the extremes in wet straining. In the most highly oriented sheet, wet straining slightly decreases the shear modulus (dashed line).

[Figure 10 here]

Determination of the in-plane Poisson ratios has been described elsewhere (7). The results here will be discussed in terms of the geometric mean of the two in-plane Poisson ratios, $(\nu_{xy}\nu_{yx})^{1/2}$. The Poisson ratios were found to be independent of apparent density in the range studied, so averages were calculated for the sheets of different apparent densities. These are presented in Table III.

[Table III here]

It is evident that the geometric mean of the Poisson ratios is reasonably constant for both random and slightly oriented sheets at all wet straining levels. For the most highly oriented sheets, however, the geometric mean is smaller, and it is dramatically reduced further with wet straining.

The constancy of $(\nu_{xy}\nu_{yx})^{1/2}$ at random and low fiber orientations, over the range of wet straining studied, agrees with results found earlier in investigations of machine-made papers (8). In the earlier work, the data for the in-plane elastic constants of machine-made papers were found to fit an approximate relationship used to describe other orthotropic systems (25), $G_{xy} \doteq (E_xE_y)^{1/2}/2\ (1 + (\nu_{xy}\nu_{yx})^{1/2})$. This expression is obtained by replacing G, E, and ν in the exact expression for an isotropic material, $G = E/2(1 + \nu)$, by the geometric means for E and ν for the orthotropic material. In the previous work, $(\nu_{xy}\nu_{yx})^{1/2}$ was also found to be almost constant, having a mean value for 30 different paper samples of 0.293 with a standard deviation of 0.023. Using this mean value, $G_{xy} \doteq 0.387\ (E_xE_y)^{1/2}$, a result which agreed well with (mechanical) data from the literature in which E_x, E_y, and G_{xy} are reported. From the present work it is clear that $(\nu_{xy}\nu_{yx})^{1/2}$ is not constant for all conditions, decreasing significantly at high fiber orientations and wet strains. The approximate relationships above do not apply to the in-plane constants for the highly anisotropic samples.

The z-direction stiffness, C_{33} (which is related to E_z), was measured ultrasonically and was found to be a strong function of the apparent density of the sheet, as shown in Figure 11. The ZD stiffness does not depend very much on the in-plane fiber orientation. The three lines in the figure correspond to the three wet straining levels. The data in Figure 11 are for the oriented sheets only. The ZD stiffness decreases dramatically with wet straining. At a constant apparent density, ZD stiffness was reduced by almost 50% by wet straining in the plane of the sheet.

[Figures 11 and 12 here]

The tensile strength in the thickness direction was measured according to the method developed by Wink and Van Eperen (26). The ZD tensile strength is also reduced by wet straining in the plane of the sheet. Although the ZD strength data exhibit more scatter than the ZD modulus data, there is a linear relationship between the z-direction tensile strength and the Z-direction stiffness as shown in Figure 12. This is analogous to the general relationship found between the tensile strength and Young's modulus in either the MD or CD in the plane of the sheet.

CONCLUSIONS

Paper may be thought of as a three-dimensional orthotropic homogeneous continuum as far as wave propagation techniques are concerned, as long as the wavelengths are large with respect to fiber dimensions. The application of orthotropic plate wave theory to paper has improved our understanding of wave propagation in paper and has led to experimental methods for determining the nine orthotropic elastic constants. These constants form a self-consistent set.

Ultrasonic measurements are normally carried out on unstrained samples. We found, however, that if ultrasonic measurements are made on sheets stressed (mechanically) to near failure, the measured elastic constants are essentially the same as those measured in the unstressed sheet case (except for corrections of the order of the strain). This suggests that the mechanisms governing the high frequency stress-strain relationships are relatively independent of those phenomena which are important in the usual, long time scale, stress-strain response. Arguments of this type explain the observed differences between "mechanical" and "ultrasonic" elastic constants, the latter typically higher by 20 to 30%.

The in-plane and out-of-plane elastic moduli, all measured by ultrasonic techniques, depend on the extent of fiber orientation, the level of wet straining, and the apparent density of the sheet. Increasing fiber orientation or wet straining increases the modulus and tensile strength in the direction of fiber orientation or straining, and concomitantly decreases the corresponding properties in the other two directions. The most dramatic effect of wet straining in the plane occurred in the thickness direction, where a moderate strain of 2.4% resulted in a 50% reduction in the ZD stiffness. On the other hand, unlike the in-plane stiffnesses, the in-plane fiber orientation had little effect on the ZD stiffness. The full importance of these observations will ultimately depend on how important the z-direction properties of paper are in determining the final converting or end use requirements of the material. In any case, it is important to realize that the effects of wet straining in the MD to gain stiffness or strength results in significant decreases in these properties in the CD and ZD.

The in-plane shear modulus, G_{xy} depends mainly on apparent density. It is reduced somewhat by increasing fiber orientation, but wet straining has no effect on the shear modulus, except at the highest fiber orientation. This observation is unexpected.

The individual in-plane Poisson ratios, ν_{xy} and ν_{yx}, are functions of fiber orientation and wet straining. The geometric mean of these, however, is relatively insensitive to fiber orientation and wet straining, at least at the lower levels of each. The value of $(\nu_{xy}\nu_{yx})^{1/2}$ does decrease significantly at the highest levels of fiber orientation and wet straining. The quantity $(\nu_{xy}\nu_{yx})^{1/2}$ may be thought of as a measure of how "interrelated" the tensions applied in one direction are to the tensions induced in another direction. Although it is conjecture, it would intuitively seem that $(\nu_{xy}\nu_{yx})^{1/2}$ should be related to paper structure. The reduction of this quantity by wet straining at high fiber orientations leads one to suspect some sort of structural damage or bond breakage. However, the stiffness and tensile strength in the MD are still increasing as a result of wet straining.

REFERENCES

1. Johnson, J. N., J. Appl. Phys. 42, 5522 (1971).
2. Habeger, C. C., Mann, R. W., and Baum, G. A., Ultrasonics 17 (2): 57 (1979).
3. Mann, R. W., Baum, G. A., and Habeger, C. C., Tappi 62 (8): 115 (1979).
4. Luukkala, M., Heikkila, P., and Surakka, J., Ultrasonics 9: 201 (1971).
5. Mann, R. W., Baum, G. A., and Habeger, C. C., Tappi 63 (2): 163 (1980).
6. Klason, C. and Kubat, J., Svensk Papperstid. 79: 494 (1976).
7. Baum, G. A. and Bornhoeft, L. R., Tappi 62 (5): 87 (1979).
8. Baum, G. A., Brennan, D. G., and Habeger, C. C. Submitted to Tappi.
9. Theory and Design of Wood and Fiber Composite Materials, (Jayne, B. A., ed.). Syracuse University Press, 1972.
10. Edge, S. R. H., Proc. Tech. Sec. P.M.A. 26: 425-431 (1945).
11. Schulz, J. H., Tappi 44 (10): 736-744 (1961).
12. Sauret, G., Techniques et Recherches Papetieres, No. 2: 3-14 (1963). (Fr.)
13. Prusas, Z. C., Tappi 46 (5): 325-330 (May, 1963).
14. Craver, J. K. and Taylor, D. L., Tappi 48 (3): 142-147 (1965).
15. Setterholm, V. C., and Chilson, W. A., Tappi 48 (11): 634-640 (1965).
16. Sauret, G., Chleq, J. P., and Lafabure, G., Technique et Recherches Papetieres No. 6: 30-40 (1965). (Fr.).

17. Taylor, D. L., and Craver, J. K., In Bolam's Consolidation of the Paper Web, Vol. 2, p. 852-72. London, Tech. Section of the Brit. Paper and Board Makers Assoc., Inc., 1966.

18. Meyers, G. C., Tappi 50 (3): 97-100 (1967).

19. Setterholm, V. and Kuenzi, E. W., Tappi 53 (10): 1915-20 (1970).

20. Parsons, S. R., Tappi 55 (10): 1516-21 (1972).

21. Matolesy, G., C.P.P.A. Annual Mtg. (Montreal) 60, Preprints Book B: 19-29 (1974).

22. Kimura, M., Karami, Y., Usuda, M., and Kadoya, T., J. Japan Wood Res. Soc. (Mokuzai Gakkaishi) 24 (10): 743-749 (1978) (Jap.).

23. Sauret, G., Bull. ATIP 16 (6): 446-454 (1962).

24. Centre Technique de l'Industrie des Papiers, Cartons et Celluloses, French patent 2,030,715 (Nov. 13, 1970).

25. Szilard, R. Theory and Analysis of Plates, Prentice-Hall Inc. Englewood Cliffs, NJ 1974.

26. Wink, W. A., and Van Eperen, R. H., Tappi 50 (8): 393-400 (1967).

TABLE I

ULTRASOUND VELOCITIES AT MAXIMUM LOAD[a]
FOR MECHANICALLY STRAINED SPECIMENS

RH, %	Load, N	Strain, %	V/V_o[b] MD Longitudinal	V/V_o CD Longitudinal	V/V_o Shear
15	712	0.46	1.026 (0.014)	0.998 (0.014)	1.012 (0.011)
48	712	0.72	1.020 (0.030)	0.994 (0.014)	1.013 (0.011)
66	623	0.74	1.037 (0.010)	0.991 (0.014)	1.010 (0.014)
80	534	0.98	1.062 (0.016)	0.981 (0.010)	1.010 (0.011)

[a]About 80% of failure load. Numbers in parentheses are standard deviations.
[b]V_o are the velocities at zero stress and zero strain for each direction and wave type at each RH condition.

TABLE II

VELOCITY RATIOS DURING STRESS RELAXATION

Time, hours	Load, N	Strain, %	Velocity Ratios, V/V_o[a] MD Longitudinal	CD Longitudinal	Shear
1	489-520	0.61	1.051	0.999	1.010
22	425-431	0.61	1.046	0.989	1.009
90	387-391	0.61	1.042	1.002	1.009
162	391	0.61	1.045	0.994	1.006
430	351	0.61	1.039	0.997	1.009

[a]V_o are the velocities at zero strain and zero stress. All measurements at 48% RH, 22.8°C.

TABLE III

THE DEPENDENCE OF $(\nu_{xy}\nu_{yx})^{1/2}$ ON FIBER ORIENTATION AND WET STRAINING

Wet Strain, %	Fiber Orientation		
	Random	Low	High
0	0.254	0.250	0.200
1.2	0.250	0.269	0.147
2.4	0.260	0.279	0.087

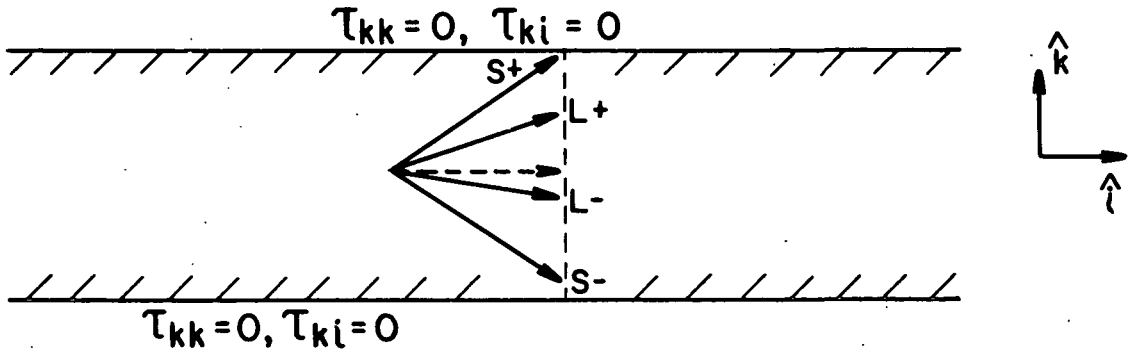

Figure 1. Construction of orthotropic plate waves from four orthotropic bulk waves.

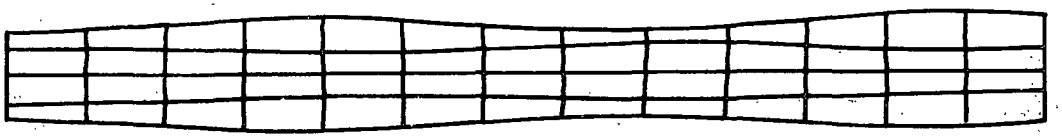

a. Symmetric mode

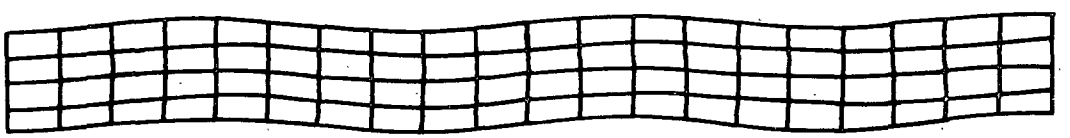

b. Antisymmetric mode

Figure 2. Two types of plate modes.

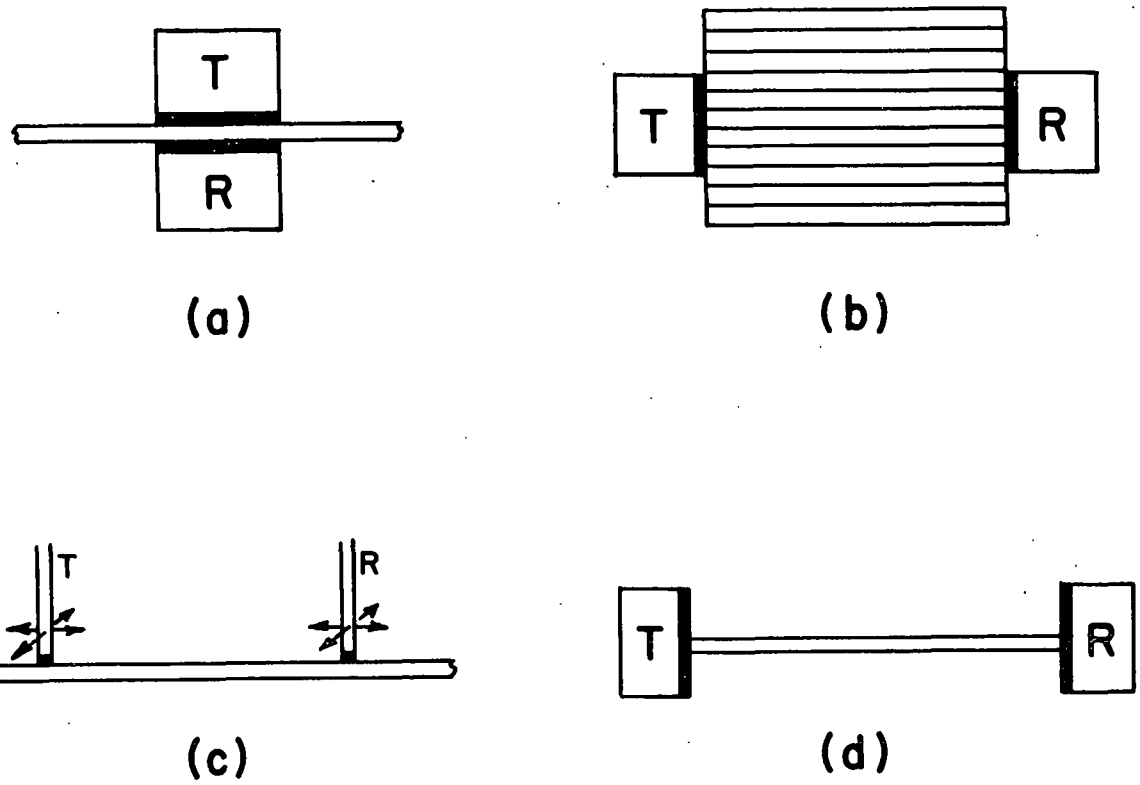

Figure 3. Transducer-specimen configurations for bulk wave measurements. (a) z-direction, L or S. (b) MD or CD measurements, L or S. (c) MD or CD measurements, L or S. (d) MD or CD measurement, L or S. T = transmitter, R = receiver, L = longitudinal, S = shear.

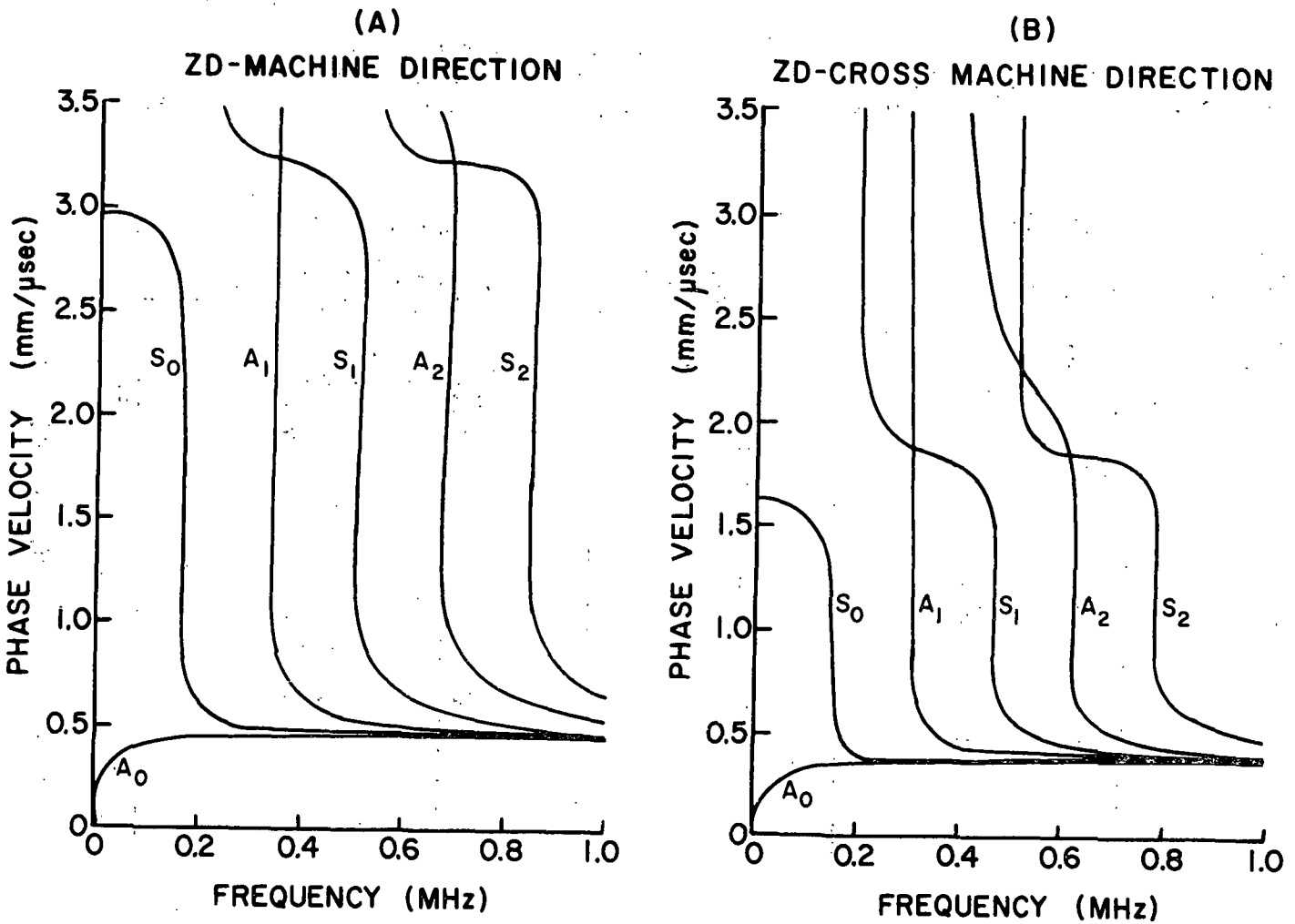

Figure 4. Orthotropic plate waves for the ZD-MD plane (A) and ZD-CD plane (B). First three modes shown for each. Calculated using measured bulk orthotropic elastic constants. (A) $C_{11}/\rho = 10.2$, $C_{13}/\rho = 0.32$, $C_{33}/\rho = 0.08$, $C_{55}/\rho = 0.22$, all in $(mm/\mu sec)^2$. (B) $C_{22}/\rho = 3.47$, $C_{23}/\rho = 0.25$, $C_{33}/\rho = 0.08$, $C_{44}/\rho = 0.16$, all in $(mm/\mu sec)^2$. Chipboard specimen of thickness 0.75 mm.

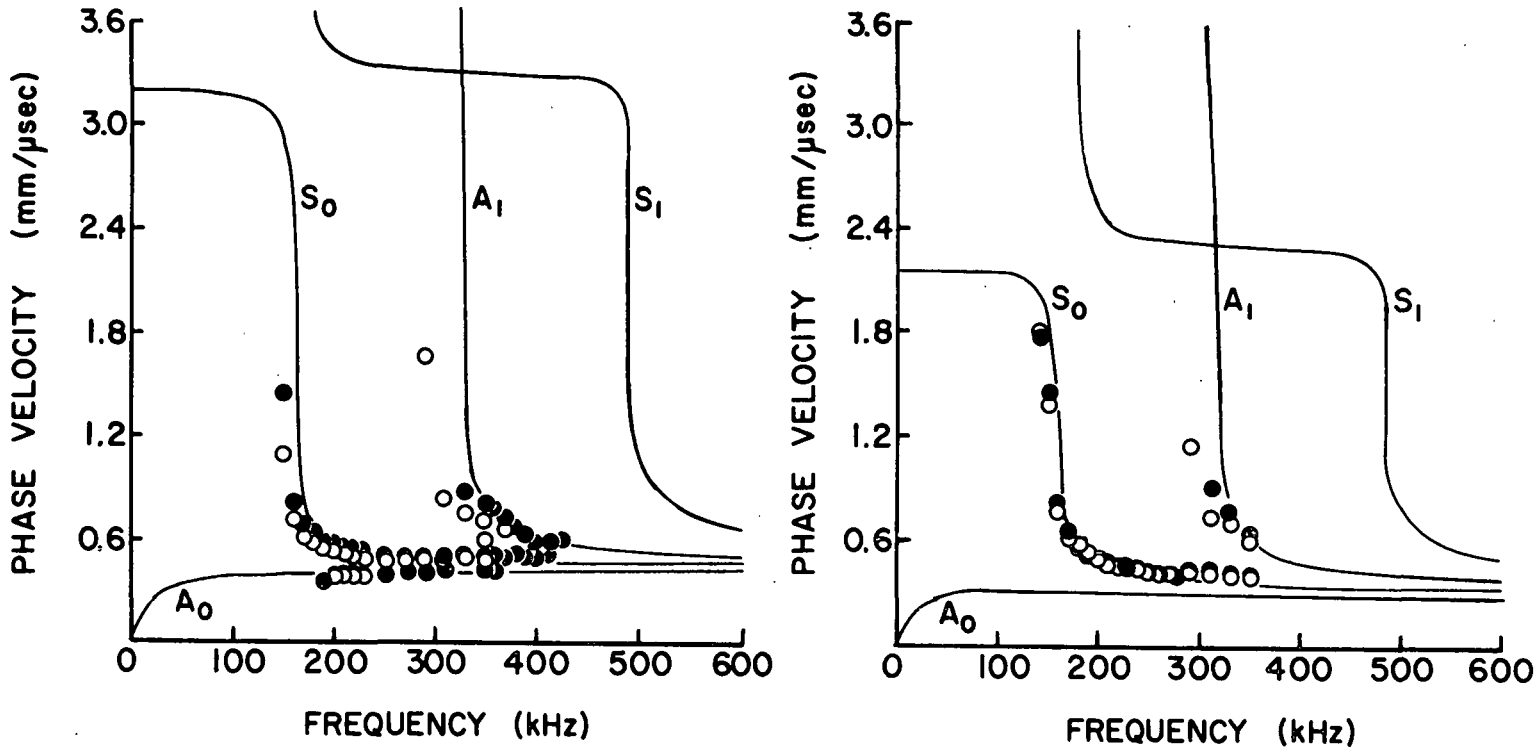

Figure 5. Comparison of measured plate wave velocities (o Specimen 1 and • Specimen 2) with curves predicted from theory and using bulk wave velocities measured on same material.

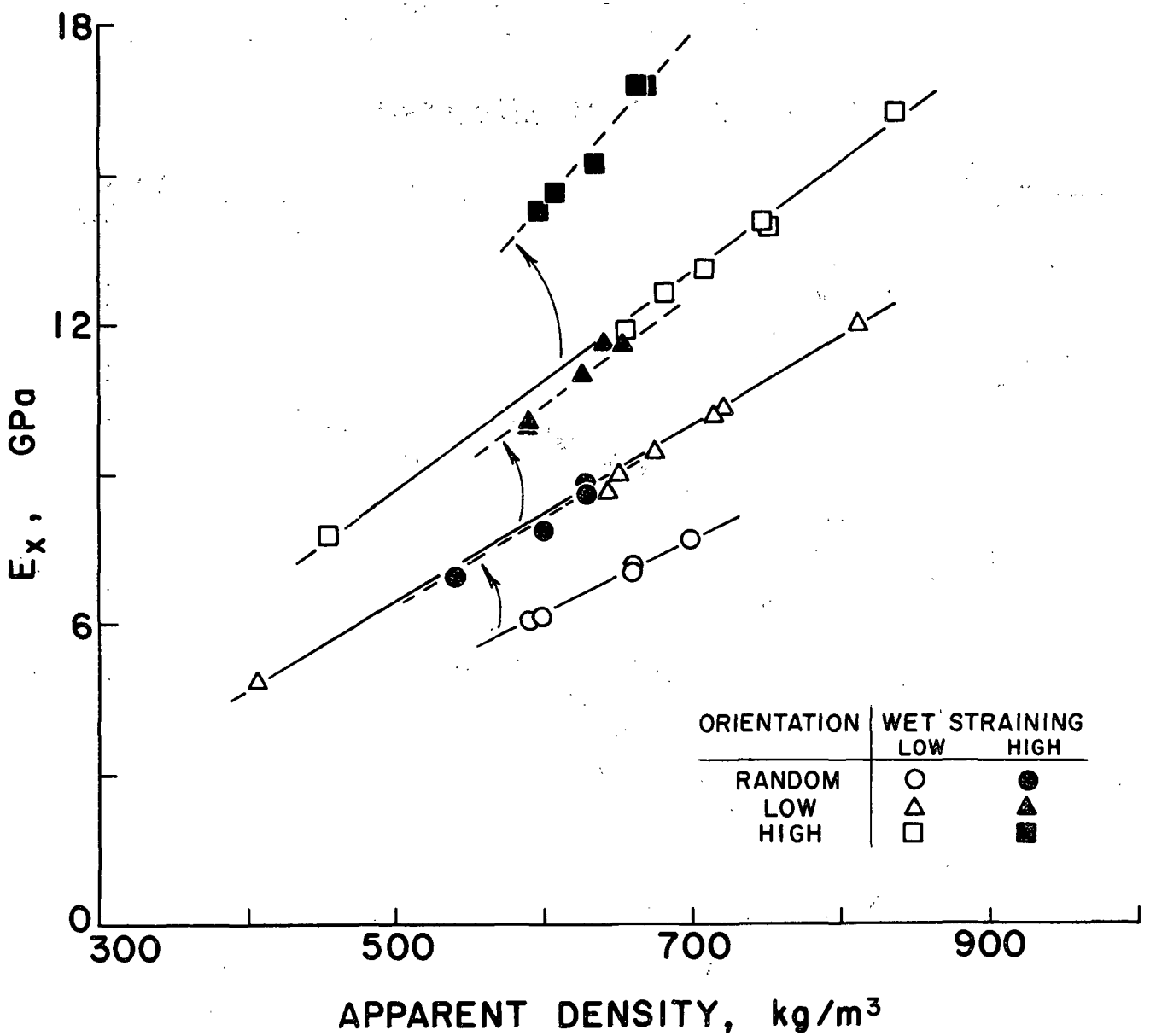

Figure 6. Young's modulus in the MD, E_x, as a function of apparent density at different fiber orientations and wet straining levels.

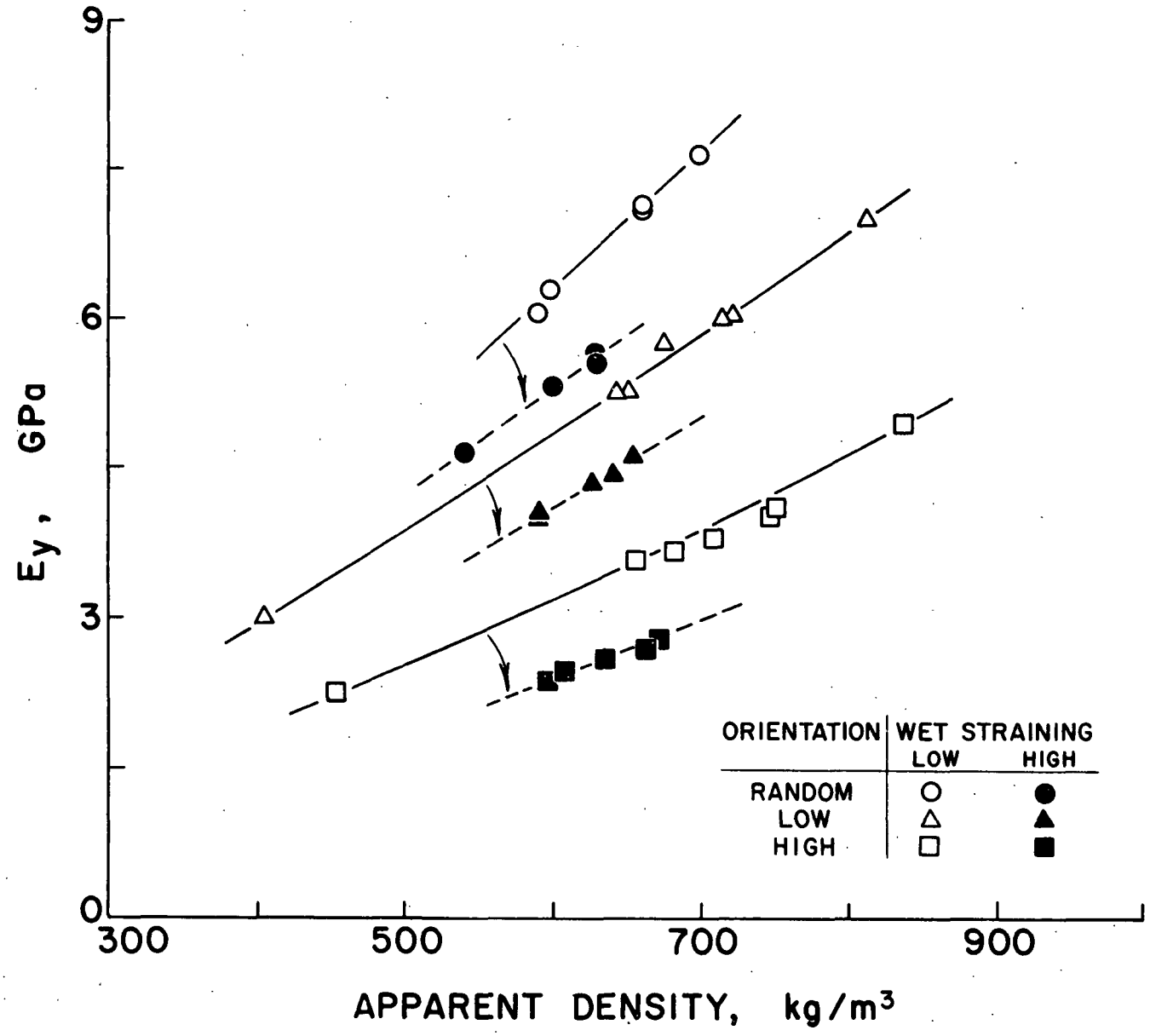

Figure 7. Young's modulus in the CD, E_y, as a function of apparent density at different fiber orientations and wet straining levels.

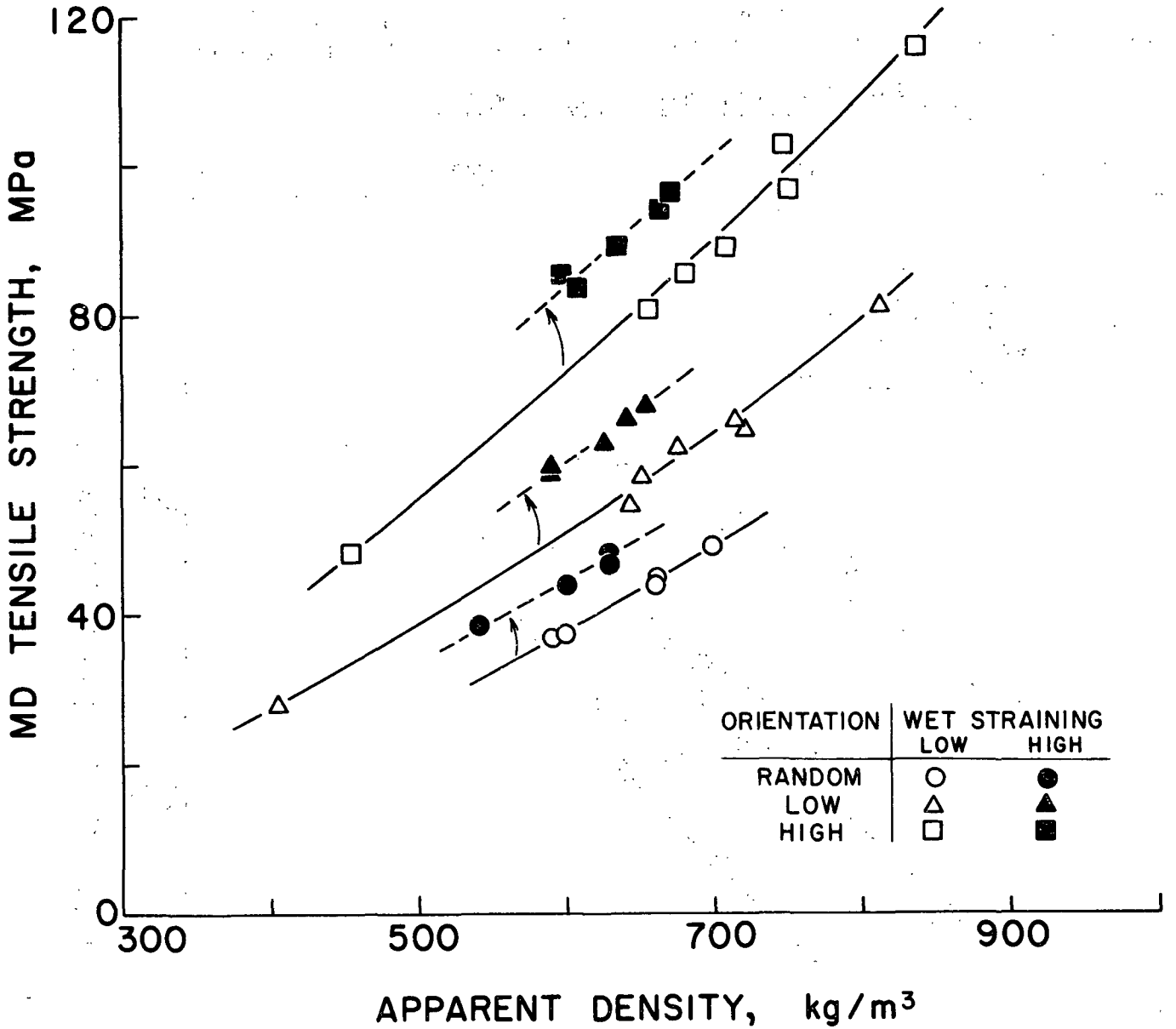

Figure 8. MD tensile strength as a function of apparent density at different fiber orientations and wet straining levels.

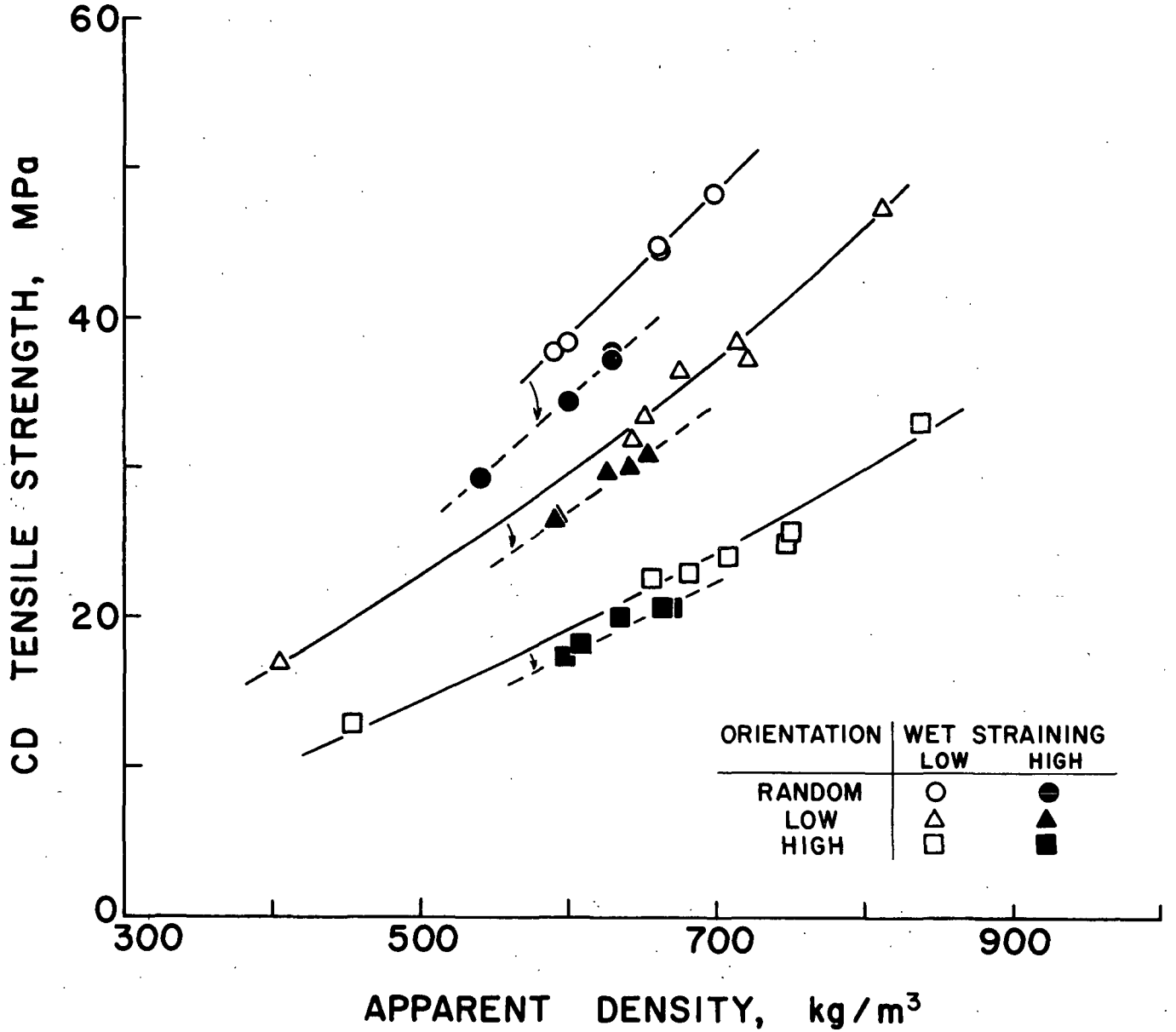

Figure 9. CD tensile strength as a function of apparent density at different fiber orientations and wet straining levels.

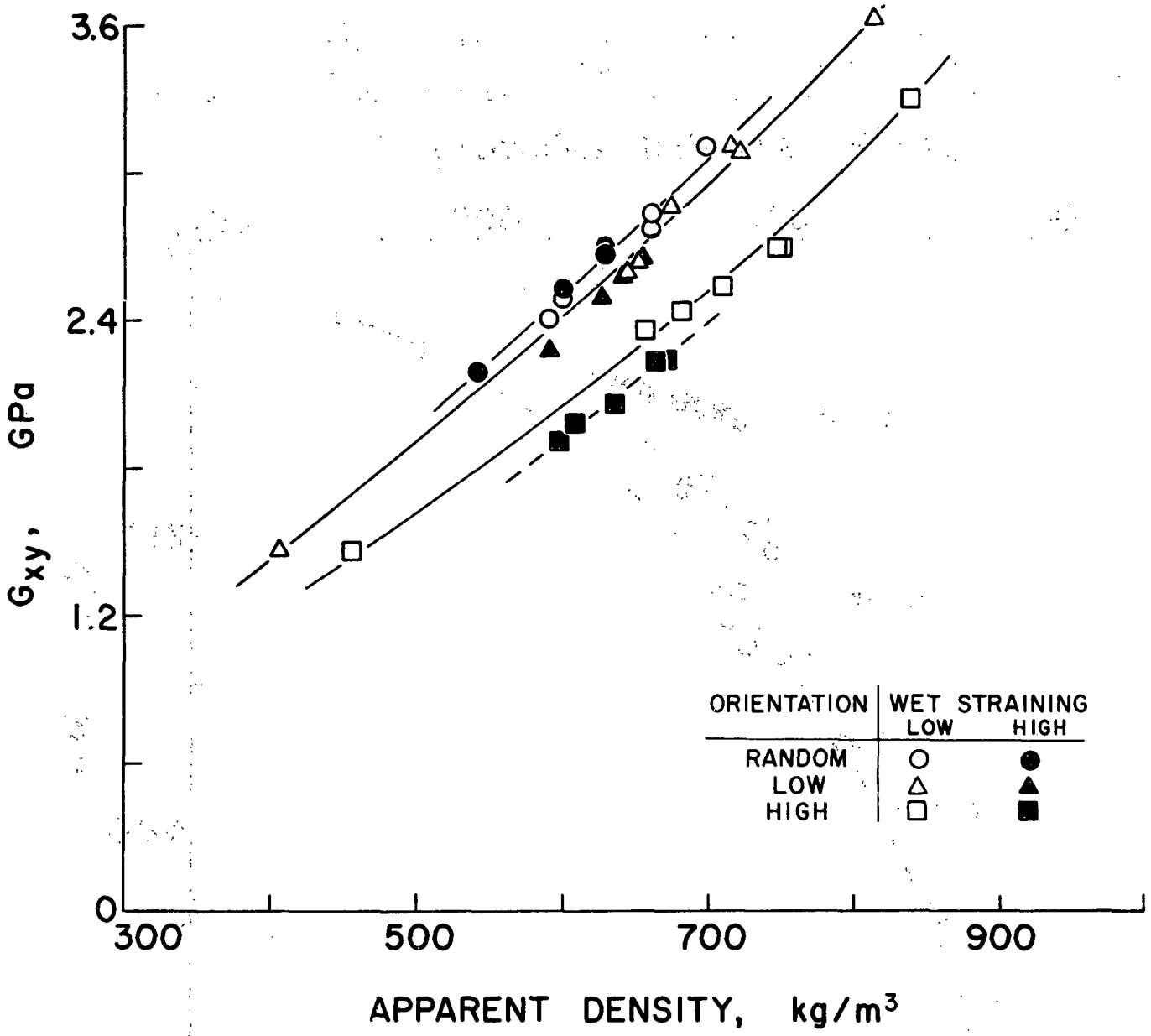

Figure 10. The in-plane shear modulus, G_{xy}, as a function of apparent density at different fiber orientations and wet straining levels.

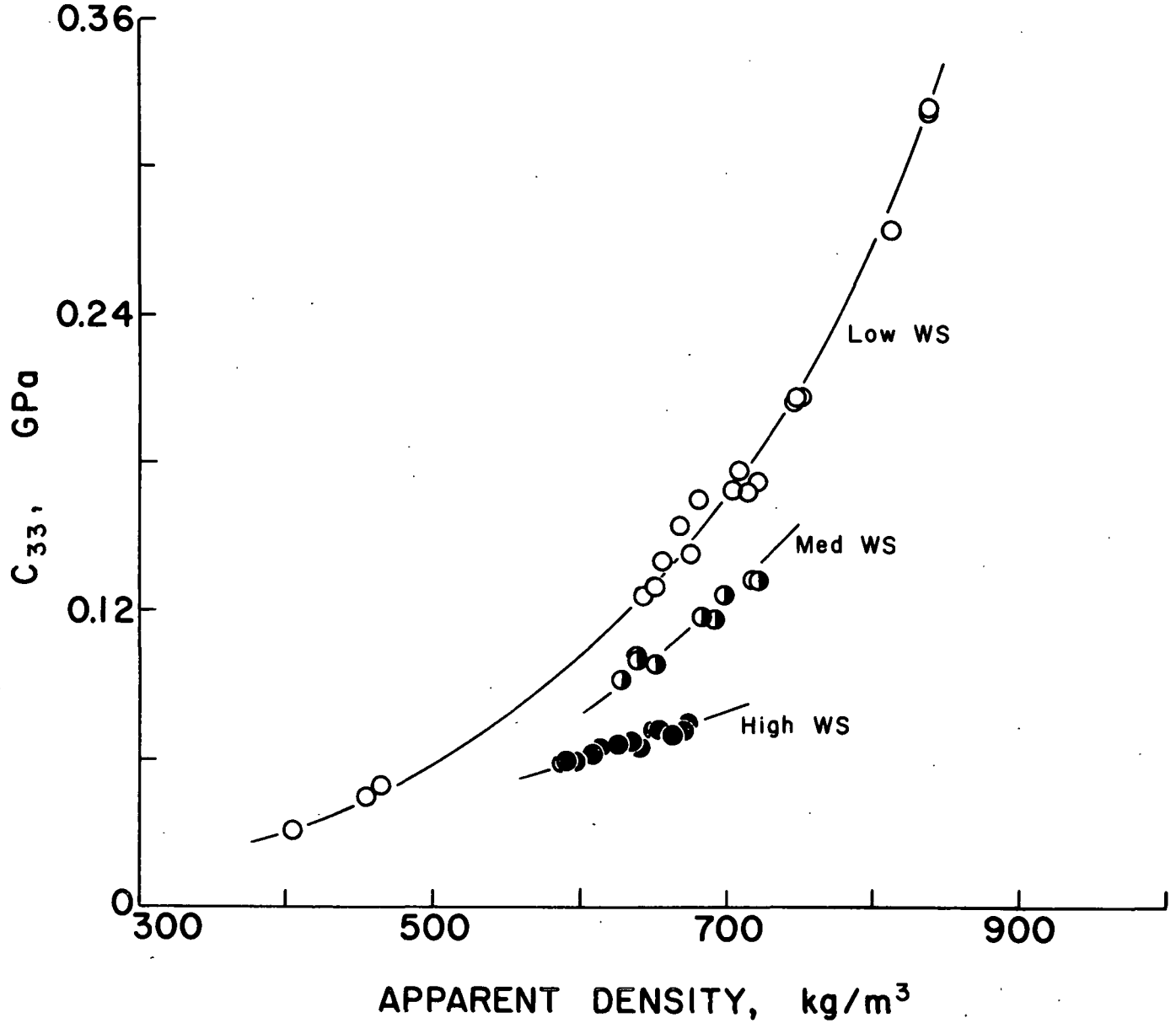

Figure 11. The ZD stiffness, C_{33} (which is related to E_z) as a function of apparent density. The three curves correspond to the three levels of wet straining: high, medium, and low. C_{33} is insensitive to fiber orientation.

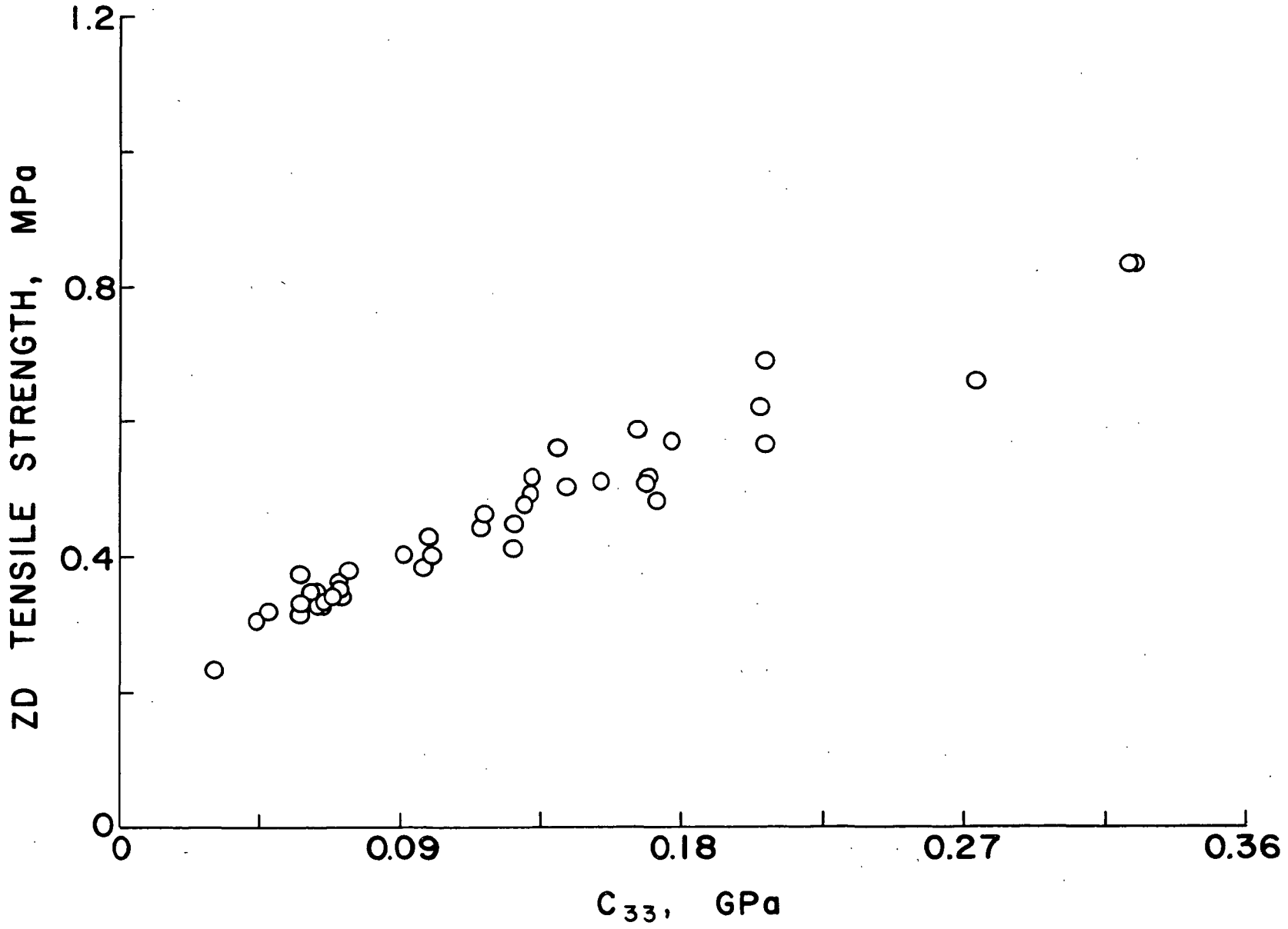

Figure 12. The ZD tensile strength versus out-of-plane elastic stiffness, C_{33}.